CONF-8311137-1
DE84 003387

A HIGH RESOLUTION ULTRASONIC DENSITOMETE

W. B. Dress

Oak Ridge National Laboratory,* Oak Ridge, T

Abstract

The velocity of torsional stress pulses in an ultrasonic waveguide of non-circular cross section is affected by the temperature and density of the surrounding medium. Measurement of the transit times of acoustic echoes from the ends of a sensor section are interpreted as level, density, and temperature of the fluid environment surrounding that section. This paper examines methods of making these measurements to obtain high resolution, temperature-corrected absolute and relative density and level determinations of the fluid. Possible applications include on-line process monitoring, a hand-held density probe for battery charge state indication, and precise inventory control for such diverse fluids as uranium salt solutions in accountability storage and gasoline in service station storage tanks.

1. Introduction

It is well known that the velocity of propagation of torsional waves in an ultrasonic waveguide of non-circular cross section is influenced by the density of the surrounding medium. Lynnworth[1], in particular, has examined this property of torsional-wave propagation in rectangular bars specifically for density and level measurements.

Some of the early hopes for high-resolution density measurements have thus far been left unrealized. The simple proposition that precise measurement of a time interval implies high resolution

diverse fluids as uranium salt solutions in accountability storage and gasoline in service station storage tanks.

1. Introduction

It is well known that the velocity of propagation of torsional waves in an ultrasonic waveguide of non-circular cross section is influenced by the density of the surrounding medium. Lynnworth[1], in particular, has examined this property of torsional-wave propagation in rectangular bars specifically for density and level measurements.

Some of the early hopes for high-resolution density measurements have thus far been left unrealized. The simple proposition that precise measurement of a time interval implies high resolution of absolute density measurements neglects the effect of signal-to-noise ratio as well as several systematic effects to be discussed below. It is the purpose of this paper to indicate how such measurements may be made in the laboratory and extended to the field in practical and reliable instrumentation.

2. Principle of operation

Modes of Propagation

The principles of acoustic stress-pulse generation and propagation in waveguides are summarized to provide an introduction to the discussion below.

---

*Operated by Union Carbide Corporation under contract W-7405-eng-26 with the U.S. Department of Energy.

The velocity of propagation of acoustic waves in an elastic medium is proportional to the square root of a restoring force (described by the elastic constants) divided by an inertial term (which is a density or a moment of inertia).[2] For the case where the transverse dimensions are much smaller than the wavelength, the transverse strain is negligible, and the elastic modulus is Young's modulus, Y. The velocity of the corresponding extensional wave is

$$v = \sqrt{Y/\rho} \quad , \qquad (1)$$

where ρ is the density of the elastic medium. If the medium supports shear, a torsional mode may be excited. The appropriate elastic modulus is the modulus of rigidity or the shear modulus, G. The velocity of the corresponding torsional wave, for a rod of circular cross section, is given by

$$v = \sqrt{G/\rho} \quad . \qquad (2)$$

Stress Pulse Generation

Extensional and torsional acoustic stress pulses can be generated in magnetostrictive materials by the Joule and Wiedemann effects, respectively.[3,4] A current pulse in a coil surrounding a ferromagnetic rod creates a magnetic-flux transient in the rod causing a change in length (Joule Effect), which propagates as an extensional wave. Conversely, a travelling stress pulse produces a local dimensional change (strain) which causes a change in magnetic flux in a ferromagnetic rod (Villari Effect), and induces a voltage in the pick-up coil surrounding the rod by Faraday's Law.

Analogously, a change in shear will propagate at the corresponding torsional velocity. Such a shear can be produced by applying an azimuthal magnetic bias; the longitudinal magnetic pulse produced in the excitation coil will then add vectorially to the azimuthal field causing the rod to shear (Wiedemann Effect). This traveling torsional pulse is detected in a manner similar to the extensional pulse, the only difference being that an azimuthal magnetic bias is required at the pick-up coil also.

Non-Circular Waveguides

For a waveguide of non-circular cross section, Eq. 2 must be modified to reflect the tendency of a solid rod to buckle when twisted. The appropriate factor is the torsional constant,[5] J, which has the effect of increasing the stiffness. The expression for the torsional velocity becomes

$$v = \sqrt{(GJ)/(\rho I)} \qquad (3)$$

where I is the polar moment of inertia of the rod about the axis of shear. Following Lynnworth in ref. 1, a geometrical shape factor, K, is defined as the ratio of the velocity in a non-circular rod to that in a circular rod of the same material:

$$K = \sqrt{J/I} \qquad (4)$$

For a circular rod, K is unity, and decreases as the shape departs from that of a circle.

Effects of Fluid Coupling

For a waveguide immersed in a fluid of density ρ, the extensional propagation is largely unaffected. However, the torsional motion of the rod can easily couple to the fluid, transferring both energy and momentum.

Lynnworth in ref. 1, quantified the velocity reduction with an empirical factor given by

$$f = 1 + \frac{\rho_f}{2\rho_f}\left(1 - \frac{1}{K}\right) \qquad (5)$$

where ρ_s is the density of the sensor, ρ_f is the fluid density. Arave[6] cautions that this expression for f is valid only for sensors with rectangular cross sections, mentioning that "shapes other than rectangular do not have as distinctive a torsional wave envelope".

An elaboration of Eq. 3 can be made as follows. The inertial term, ρI includes the contribution of the fluid, in the general manner

the shape departs from that of a circle.

Effects of Fluid Coupling

For a waveguide immersed in a fluid of density ρ, the extensional propagation is largely unaffected. However, the torsional motion of the rod can easily couple to the fluid, transferring both energy and momentum.

Lynnworth in ref. 1, quantified the velocity reduction with an empirical factor given by

$$f = 1 + \frac{\rho_f}{2\rho_f}\left(1 - \frac{1}{K}\right) \qquad (5)$$

where ρ_s is the density of the sensor, ρ_f is the fluid density. Arave[6] cautions that this expression for f is valid only for sensors with rectangular cross sections, mentioning that "shapes other than rectangular do not have as distinctive a torsional wave envelope".

An elaboration of Eq. 3 can be made as follows. The inertial term, ρI includes the contribution of the fluid, in the general manner

$$\rho_s I = \rho_s I\,[1 + F(\rho)] \qquad (6)$$

where ρ is the fluid density, and F is the ratio of the "inertial" contribution of the fluid to that of the sensor. The general expression for the velocity reduction factor, f, of Eq. 5 is

$$f = [1 + F(\rho)]^{-1/2} \quad . \qquad (7)$$

3. Experimental method

Torsional pulses were generated in both nickel tubing and an iron-cobalt alloy. To switch modes from torsional to extensional for the temperature measurements, a means of providing both azimuthal and longitudinal magnetic bias fields was used. A further benefit of the torsional bias field was the ability to control the amplitude of the torsional signal; when the transducer is near magnetic saturation in the azimuthal direction, the generation of extensional waves is greatly reduced, and vice

versa. Thus the measurement cycle evolved into a three step process: turn on the torsional bias (a dc current passing through the transducer rod) and make the torsional (density-dependent) determination; switch to the extensional bias (dc coils wound over or along side of the pick-up coil) and make the extensional (temperature-dependent) measurement; demagnetize the transducer by applying an ac current of diminishing amplitude to the extensional bias coils to be ready for the next torsional bias application. This particular sequence is due to the recognition that a longitudinal magnetic field in a rod is much easier to maintain than an azimuthal field; demagnetization before the extensional cycle accomplishes little, but residual magnetization after the measurement would permit a significant extensional signal during the subsequent torsional cycle, dividing the pulse energy between the two modes and complicating the interpretation of the echo pattern.

The equipment used to carry out the above prescription is indicated in Fig. 1. For high resolution tests, the microcomputer and counters were replaced with an oscilloscope having a time resolution of 1 ns; this was not as restrictive as the 250 ns resolution of the microcomputer's clock. Plans for a future instrument incorporate a 100 MHz clock and high-speed counters into a microprocessor-based device which will be capable of carrying out the temperature correction and interpretation of multi-sectioned sensors as to temperature, level, density, and void-fraction information. The resulting multivariable output from a single sensor gives the user a powerful process-monitoring tool for displaying and recording the sensor's environment. Indeed, the currently implemented computer-based version accomplishes all of these measurements and operator control as well ~~albeit at a much lower resolution.~~

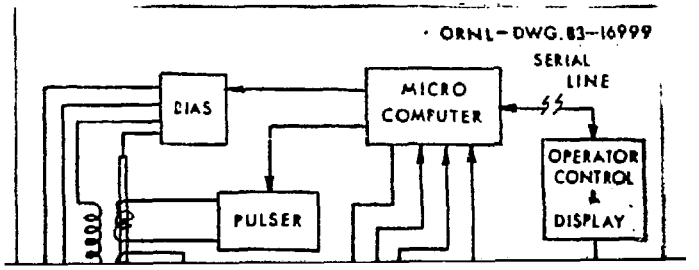

tion tests, the microcomputer and counters were replaced with an oscilloscope having a time resolution of 1 ns; this was not as restrictive as the 250 ns resolution of the microcomputer's clock. Plans for a future instrument incorporate a 100 MHz clock and high-speed counters into a microprocessor-based device which will be capable of carrying out the temperature correction and interpretation of multi-sectioned sensors as to temperature, level, density, and void-fraction information. The resulting multivariable output from a single sensor gives the user a powerful process-monitoring tool for displaying and recording the sensor's environment. Indeed, the currently implemented computer-based version accomplishes all of these measurements and operator control as well~~, albeit at a much lower resolution.~~

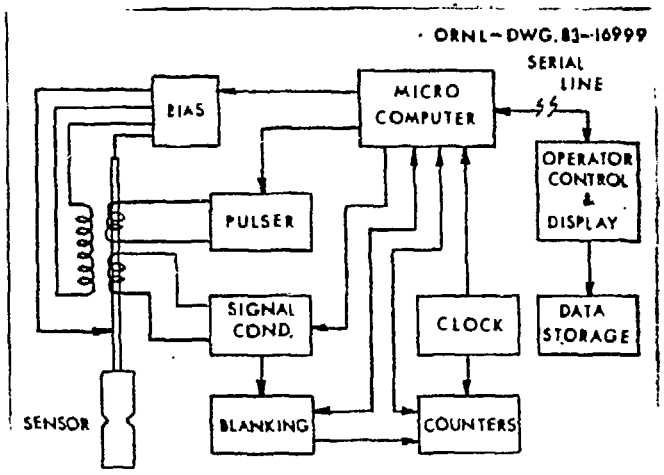

Figure 1 - Block Diagram of Equipment To Measure Level and Density.

Temperature Effects

The temperature variation of transit times due to changes in sensor length, density, and elastic moduli requires careful calibration for a particular piece of probe material if high-resolution measurements are to be made over a range of temperatures. In an actual application to measure density, the extensional transit time is obtained, the temperature inferred from the calibration table, and

the torsional data corrected. If temperature information is not required, the torsional times need only be obtained as a function of the extensional times at a number of arbitrary points throughout the temperature range. This is equivalent to a measurement of Poisson's ratio as a function of temperature.

Basic Sensor Design

The sensitivity of a sensor depends upon the ratio of the fluid density to the density of the sensor material, and the coupling to the fluid. Sensitivity is also directionally proportional to sensor length, and inversely proportional to the shape factor. A sensitive sensor would be made from low density material shaped to minimize K.

Some of the commercial plastics meet the requirements of low density and low acoustic attenuation. These can be easily shaped into some of the more complex shapes as triangle, tear drop, and star which exhibit low values of K.

The lack of a complete theory to quantify the fluid effect does not prevent the use of the device for high-resolution measurements. A correct theoretical expression of the velocity of torsional acoustic propagation in arbitrarily shaped waveguides will probably be difficult to obtain, and involve solving the complete non-linear partial differential equations in a vessel with finite boundaries, perhaps allowing for coupling to other modes of propagation.

Measurement Procedure

The velocity measurements were made by measuring the time delay between acoustic echos from discontinuities (depicted as notches in Fig. 1) known distances apart along the sensor's length. Typical echoes had a width of 3 to 12 μs measured at half amplitude, with a corresponding wavelength of 10 to 40 mm. The measurement problem then became one determining the time position of the relevant echo. This was taken to be the peak position; so the problem of high-resolution, precise measurements became one of determining the position of a peak to within a few parts per thousand of its width, which is possible only as long as distorting effects from nearby peaks and coupling to the

star which exhibit low values of K.

The lack of a complete theory to quantify the fluid effect does not prevent the use of the device for high-resolution measurements. A correct theoretical expression of the velocity of torsional acoustic propagation in arbitrarily shaped waveguides will probably be difficult to obtain, and involve solving the complete non-linear partial differential equations in a vessel with finite boundaries, perhaps allowing for coupling to other modes of propagation.

Measurement Procedure

The velocity measurements were made by measuring the time delay between acoustic echos from discontinuities (depicted as notches in Fig. 1) known distances apart along the sensor's length. Typical echoes had a width of 3 to 12 μs measured at half amplitude, with a corresponding wavelength of 10 to 40 mm. The measurement problem then became one determining the time position of the relevant echo. This was taken to be the peak position; so the problem of high-resolution, precise measurements became one of determining the position of a peak to within a few parts per thousand of its width, which is possible only as long as distorting effects from nearby peaks and coupling to other modes of propagation were kept small.

For density measurements, liquids of various densities were obtained by mixing two manometer oils, and weighing a known volume of the mixture. The error inherent in this procedure was determined to be 0.2%. Distilled water was also a calibration liquid, having a density of 0.9976 at 23°C; the volumetric method was verified by consistently producing a water density of 0.998 to within the expected error.

The shape factor was measured by determining both the torsional and extensional velocities for the sensor considered. The torsional velocity in the corresponding round rod was inferred from a knowledge of Poisson's ratio for the material in question (see ref. 2 for relevant tables and a definition of Poisson's ratio).

4. Results

Shape Factors and Sensitivities

A program for obtaining a numerical solution to Poisson's equation was used to compute values of the shape factor K for a variety of cross sections. Sensors with the shapes close to those used in the calculations were fabricated, and the shape factors determined from measurements of the torsional and extensional transit times as described above. The values obtained were within 10% of those calculated for a wide variety of shapes (semi-circle, triangle, tear-drop). Measurements of K obtained for rectangles agree with the calculated values to within 3% for a range of shapes from 1- × 12-mm to 1- × 1-mm.

Although the agreement of the calculated K with the measured values was quite good considering the precision in fabricating the various shapes, the calculation of sensitivity to immersion in water (based on Eq. 5 for f), while agreeing closely (within 1%) for rectangles, gave large discrepencies for the other shapes. For a tear-drop sensor with a measured K of 0.49 (the velocity was 1.53 mm/μs), the increase in transit time upon immersion in water was expected to be 7%; whereas the actual value obtained is closer to 16%. Thus the static geometry of the sensor expressed in the shape factor does not provide a complete description of the sensor's behavior. It is anticipated that inclusion of dynamic behavior of a non-rectangular rod under torsion will be able to account for this descrepency.

Temperature Effects

Series stainless steel behaves nearly linearly with respect to the square of the transit times, and can be described by a coefficient of +0.0004 per °C to within 10% for both the extensional and torsional waves over a range from 20° to 400°C. Figure 2 shows data from an oven calibration of a stainess-steel sensor. Temperature variations during the density measurements were small enough to be safely ignored.

water (based on Eq. 5 for f), while agreeing closely (within 1%) for rectangles, gave large discrepencies for the other shapes. For a teardrop sensor with a measured K of 0.49 (the velocity was 1.53 mm/μs), the increase in transit time upon immersion in water was expected to be 7%; whereas the actual value obtained is closer to 16%. Thus the static geometry of the sensor expressed in the shape factor does not provide a complete description of the sensor's behavior. It is anticipated that inclusion of dynamic behavior of a non-rectangular rod under torsion will be able to account for this descrepency.

Temperature Effects

Series stainless steel behaves nearly linearly with respect to the square of the transit times, and can be described by a coefficient of +0.0004 per °C to within 10% for both the extensional and torsional waves over a range from 20° to 400°C. Figure 2 shows data from an oven calibration of a stainess-steel sensor. Temperature variations during the density measurements were small enough to be safely ignored.

Figure 2 - Normalized Torsional Transit Times Versus Extensional Times With Temperature as a Parameter.

High Resolution Density Measurements

Figure 3 is a plot of velocity as a function of the fluid density obtained with a 170-mm-long, triangular-shaped sensor with a base of 1 mm and height of 3 mm; and a 50-mm-long tear-drop sensor with similar dimensions (the base of the triangle being rounded). For the triangle, velocity in air was found to be 1.66 mm/μs, and the shape factor, K determined to be 0.53.

Both curves exhibit non-linear behavior, so any expression for the velocity ratio is not a simple function of the density as in Eq. 5. However, for the 170-mm probe, a fit to the expression

$$(t_o/t) = 1 + A\rho + B\rho \ , \qquad (9)$$

Figure 3 - Normalized Torsional Transit Times Versus Fluid Density.

where ρ is the fluid density, results in

$$A = -0.11758, \quad B = 0.01288. \qquad (10)$$

This value of A can be identified, within the error

Figure 3 - Normalized Torsional Transit Times Versus Fluid Density.

where ρ is the fluid density, results in

$$A = -0.11758, \quad B = 0.01288. \tag{10}$$

This value of A can be identified, within the error of determination of K for the probe in question, with

$$A = (1 - 1/K)/2\rho \ , \tag{11}$$

in a manner analogous to Eq. 5. The non-linear effect (non-zero B) is not fully understood. A fit to the data obtained with the 50-mm sensor showed a larger second-order term. Indeed, the ratio of the size of the quadratic term in the two cases is very close to the ratio of the estimated wavelengths divided by the sensor lengths, giving credance to the supposition that the wavelength of the sampling pulse affects the observed echo transit times.

This lack of agreement with the empirical expression for f is not a serious drawback in making high-resolution density and level measurements. The mean value of the residual (difference of the measured density to that using Eq. 9) implies that the absolute error for density measurements is 0.0022 gm/ml over the range of 0.80 to 3.0 gm/ml.

Level Measurements

Similar considerations apply to level determination. If the pulse propagation in a partially immersed sensor is influenced by the fluid environment of approximately a wavelength long, the expression for the fractional immersion depth is given by

$$x = f\,(t/t_o - 1), \qquad (12)$$

where f is given by Eq. 7 for arbitrary shapes.

The errors in level determination are similarly about 0.22% for the probe described by the empirical curve presented in Eq. 9.

5. Conclusions

The agreement between geometrical calculations and measurements of the shape factor indicates that the static theory is well understood. The fact of close agreement between Lynnworth's f to within 1.0% over a range of densities from 1 to nearly 3 for rectangular probes, and large discrepencies for other shapes show that the dynamic theory of the coupling of the torsional motion to the fluid, and perhaps other propagation modes in the sensor, is still largely unexplained.

A more precise knowledge of the calibration densities would improve the method to better than a 0.1% error in absolute density determination. Indeed, relative changes in density are simple to detect at the 10 ns level in transit time. When measured with the 170-mm triangular probe, this implies a relative density determination to within 0.05%. A test done to this level of sensitivity, by adding 0.5 gm of a liquid of density 2.930 to 90 gm of fluid of 2.396, showed a shift of 32 ± 10 ns, which indicated a relative change in density of 0.13 ± 0.05%, which was the error expected based on the time-measurement accuracy and the weight of the added fluid.

References

The agreement between geometrical calculations and measurements of the shape factor indicates that the static theory is well understood. The fact of close agreement between Lynnworth's f to within 1.0% over a range of densities from 1 to nearly 3 for rectangular probes, and large discrepencies for other shapes show that the dynamic theory of the coupling of the torsional motion to the fluid, and perhaps other propagation modes in the sensor, is still largely unexplained.

A more precise knowledge of the calibration densities would improve the method to better than a 0.1% error in absolute density determination. Indeed, relative changes in density are simple to detect at the 10 ns level in transit time. When measured with the 170-mm triangular probe, this implies a relative density determination to within 0.05%. A test done to this level of sensitivity, by adding 0.5 gm of a liquid of density 2.930 to 90 gm of fluid of 2.396, showed a shift of 32 ± 10 ns, which indicated a relative change in density of 0.13 ± 0.05%, which was the error expected based on the time-measurement accuracy and the weight of the added fluid.

References

1. L. C. Lynnworth, IEEE Ultrasonics Symposium Proc., Cat #77CH1264-ISU, pp 29-34, 1977.

2. American Institute of Physics Handbook, Third Edition. D. E. Gray et al., editors, American Institute of Physics, McGraw-Hill Book Company, New York, 1972.

3. Richard M. Bozorth, "Ferromagnetism", D. Van Nostrand Company, Inc., New York, 1951.

4. N. S. Tsannes, IEEE Transactions on Sonics and Ultrasonics, Vol SU-13, No 2 pp 33-14, July 1966.

5. Chi-teh Wang, Applied Elasticity, McGraw Hill, New York 1953. Chapter 5.

6. A. E. Arave,"Ultrasonic Densitometer Development", in IEEE Ultrasonic Symposium Proc., Cat #79CH1482-9, Sept. 1979.